

Electronic Supplementary Information

Solventless polyester synthesis using a recyclable biocatalyst magnetic nanoarchitecture

Francesco Papatola¹, Sawssen Slimani^{1,2}, Filippo Fabbri³, Georg M. Guebitz^{3,4}, Davide Peddis^{1,2,*}, Alessandro Pellis^{1,*}

¹Università di Genova, Dipartimento di Chimica e Chimica Industriale, Via Dodecaneso 31, 16146, Genova, Italy.

²CNR, Istituto di Struttura della Materia, nM2-Lab, Monterotondo Scalo (Roma), 00015, Italy.

³Department of Agrobiotechnology, Institute of Environmental Biotechnology, University of Natural Resources and Life Sciences, Vienna, Konrad Lorenz Strasse 20, 3430 Tulln an der Donau, Austria

⁴Austrian Centre of Industrial Biotechnology, Konrad Lorenz Strasse 20, 3430 Tulln an der Donau, Austria

*Correspondence to: Prof. Davide Peddis, email: davide.peddis@unige.it and Prof. Alessandro Pellis, email: alessandro.pellis@unige.it

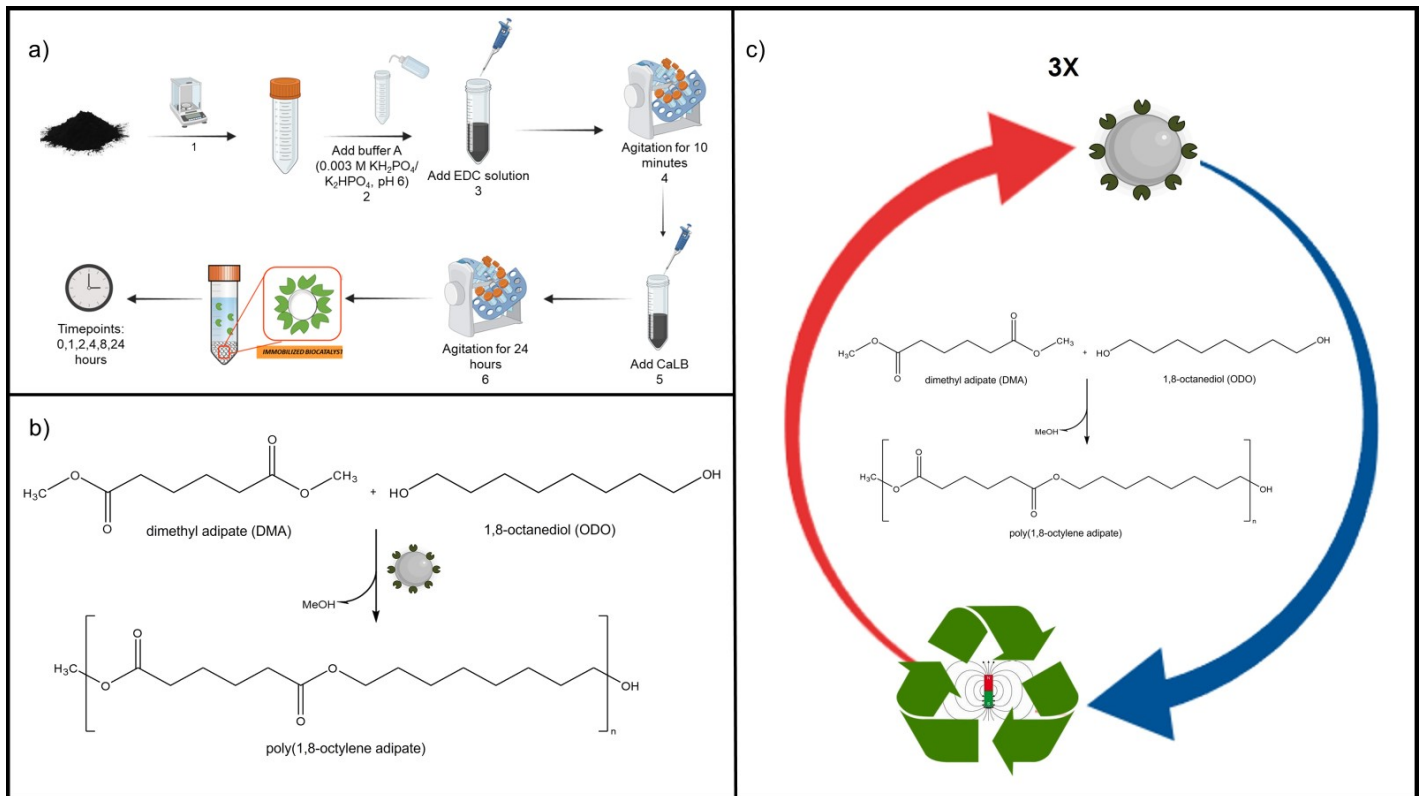


Figure S1: Schematic image for overall procedures including Immobilization of Lipase on MNPs (a), polycondensation (b) and enzyme recyclability (c)

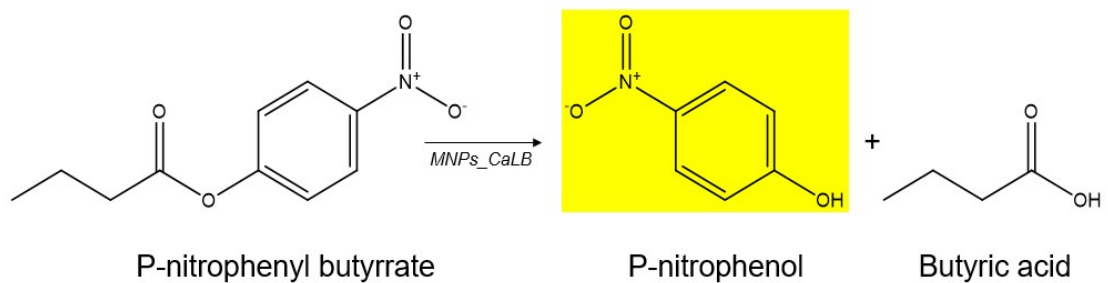


Figure S2: Schematic representation of esterase activity assay.

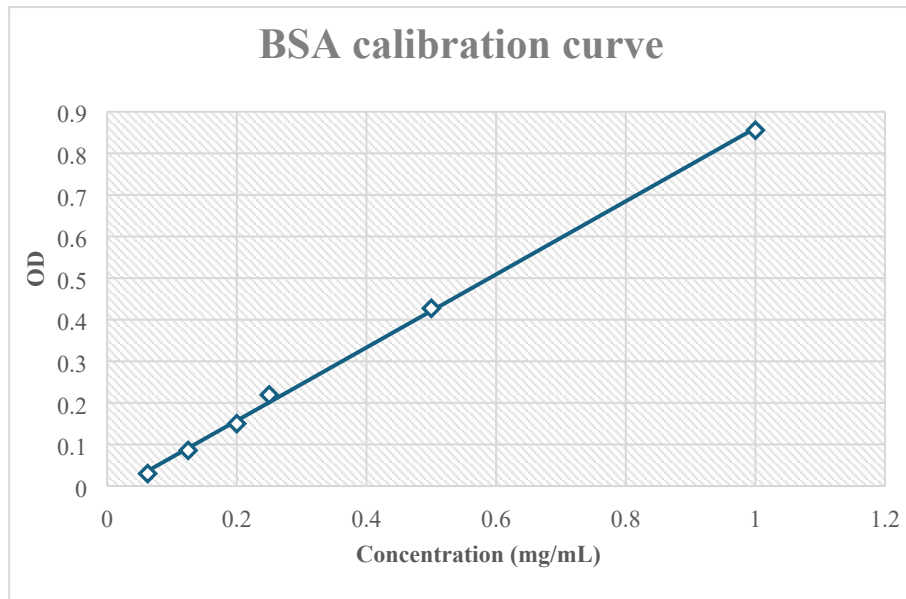


Figure S3: BSA calibration curve.

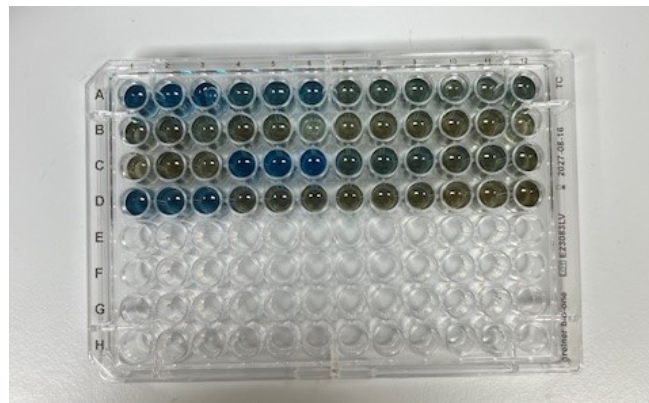


Figure S4: 96-well microtiter plate for protein concentration quantification for the different timepoint (0,1,2,4,8 and 24 h of immobilization).

From the IR analysis, we suppose that EDC reacts with MNPs to form an active urea derivative intermediate (MNPs_EDC) that is easily displaced by nucleophilic attack from CaLB functional groups in the reaction mixture and the EDC by-product is released as visible from the IR spectra where the characteristic absorption band of MNPs_EDC (C-H at 2970 cm^{-1} ; C-N at 1465 cm^{-1}) disappears in the BMN spectrum and just the absorption band related to the two typical amide bond transitions at 1630 cm^{-1} (amide I region) and 1540 cm^{-1} (amide II region) and the absorption band of CaLB associated with the σ -type C-O (typical of aa residues) at around 1036 cm^{-1} are visible. This absorption band is not present in bare MNPs spectrum confirming the binding of CaLB to MNPs.

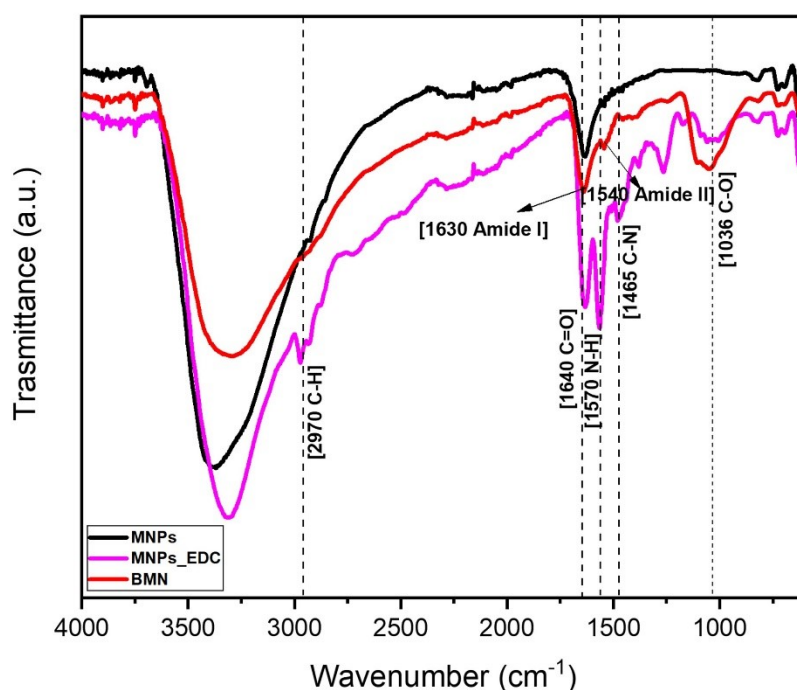


Figure S5: FTIR-ATR spectra in the range 4000 – 600 cm^{-1} of bare MNPs (black), BMN (red) and MNPs_EDC (purple).

TGA analysis of MNPs before and after Lipase immobilization was performed. Compared to MNPs, BMN presents a weight loss of 10% as a percentage of the enzyme loading. At the initial stage, the mass of BMN was almost 97% when the temperature was raised to 100 °C, indicating a slight mass loss due to the evaporation of water. The second mass loss stage occurred at approximately 200 °C, corresponding to the decomposition of the organic components (C, H, O, and N) in the enzyme conformation¹. The TG curve of BMN is similar to what was previously proven for nano-fructosome encapsulated CaLB enzyme particles by Jang et al².

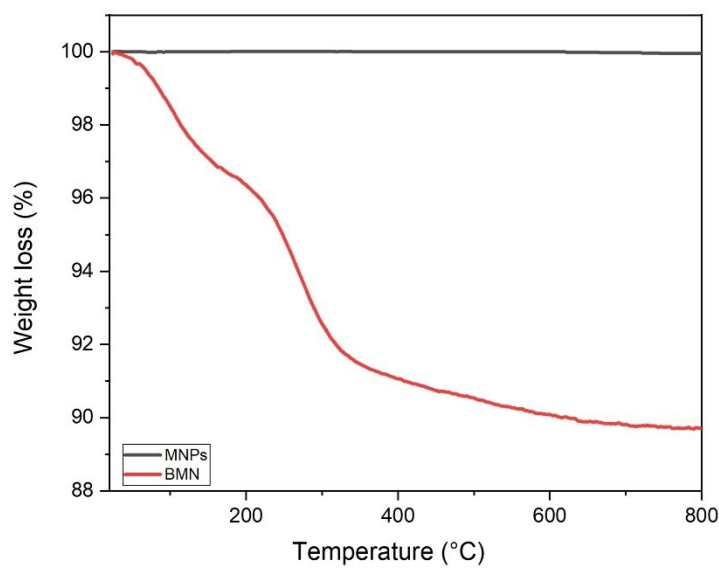


Figure S6: TGA curve of bare MNPs (black) and BMN (red)

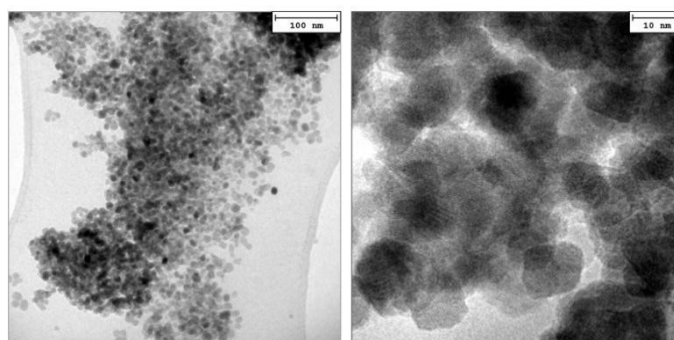


Figure S7: Transmission electron micrographs of magnetic nanoparticles at different magnification

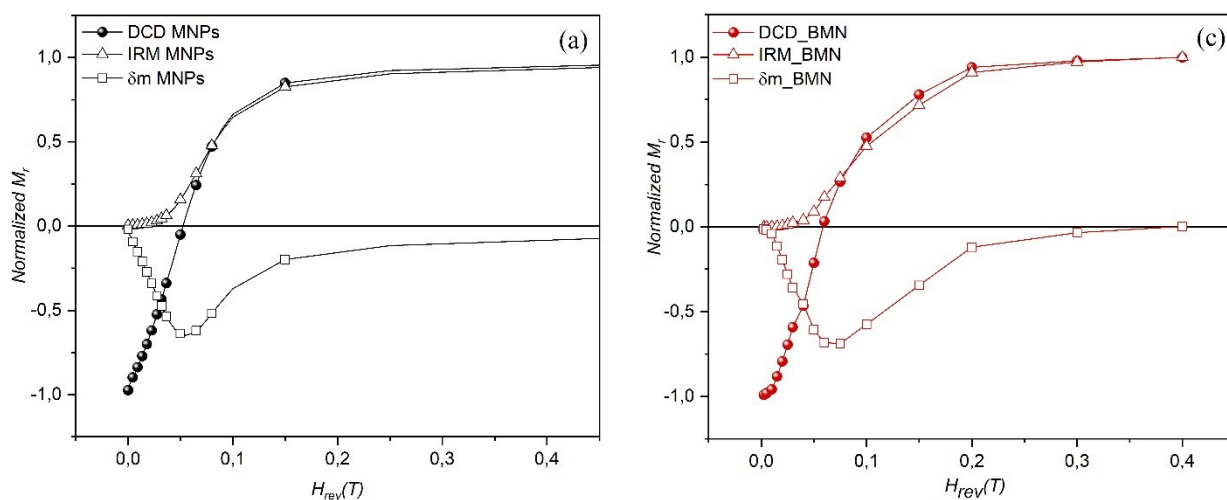


Figure S8: M_{DCD} (empty triangles), M_{IRM} (full 3D circles) and δm plot (empty squares) remanence magnetization for MNPs (a) and BMN (c) samples product

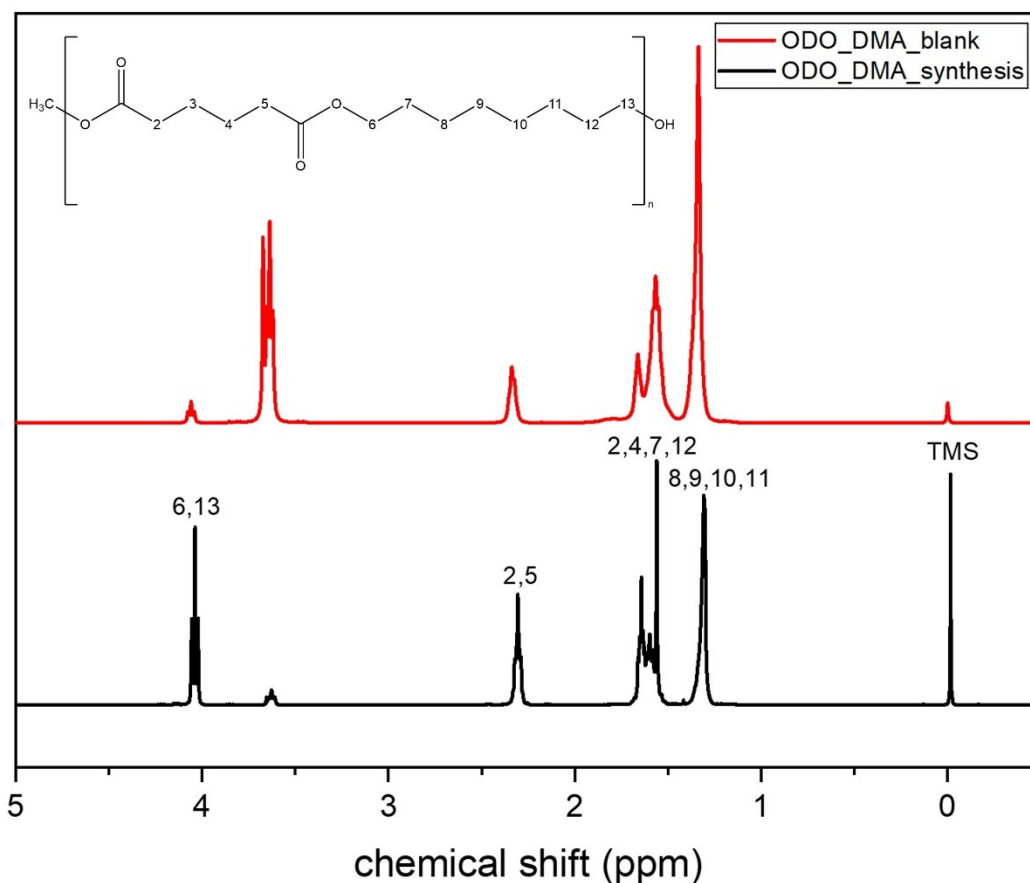


Figure S9: Comparison of 1H -NMR spectra of poly(1,8-octylene adipate) synthesized using dimethyl adipate (DMA) and 1,8-octanediol (ODO) as building blocks with BMN (ODO_DMA_synthesis) and naked MNPs (ODO_DMA_blank)

Homemade recovery system (Figure S7) has been realized inserting a commercial permanent magnet inside a glass tube; once put the tube inside the 25-mL round bottomed flask, BMN was attracted in few seconds towards the magnet and recovered for a new cycle of reaction. In the following the characteristic of commercial permanent magnet
Material/grade: NdFeB / 42MGOe Height(H) = 10 mm , Outer diameter(D) = 10 mm Flux density inside the magnet = 1.28 Tesla max. operation temperature = 180°C

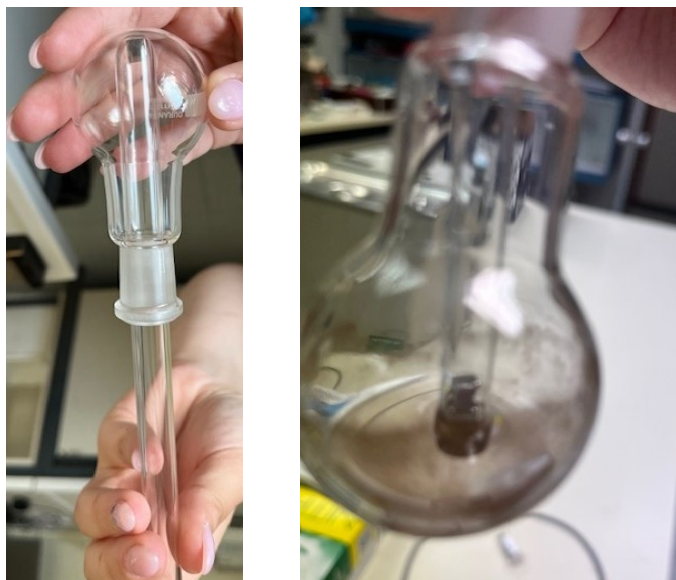


Figure S10: Recovery system to separate biocatalyst from reaction

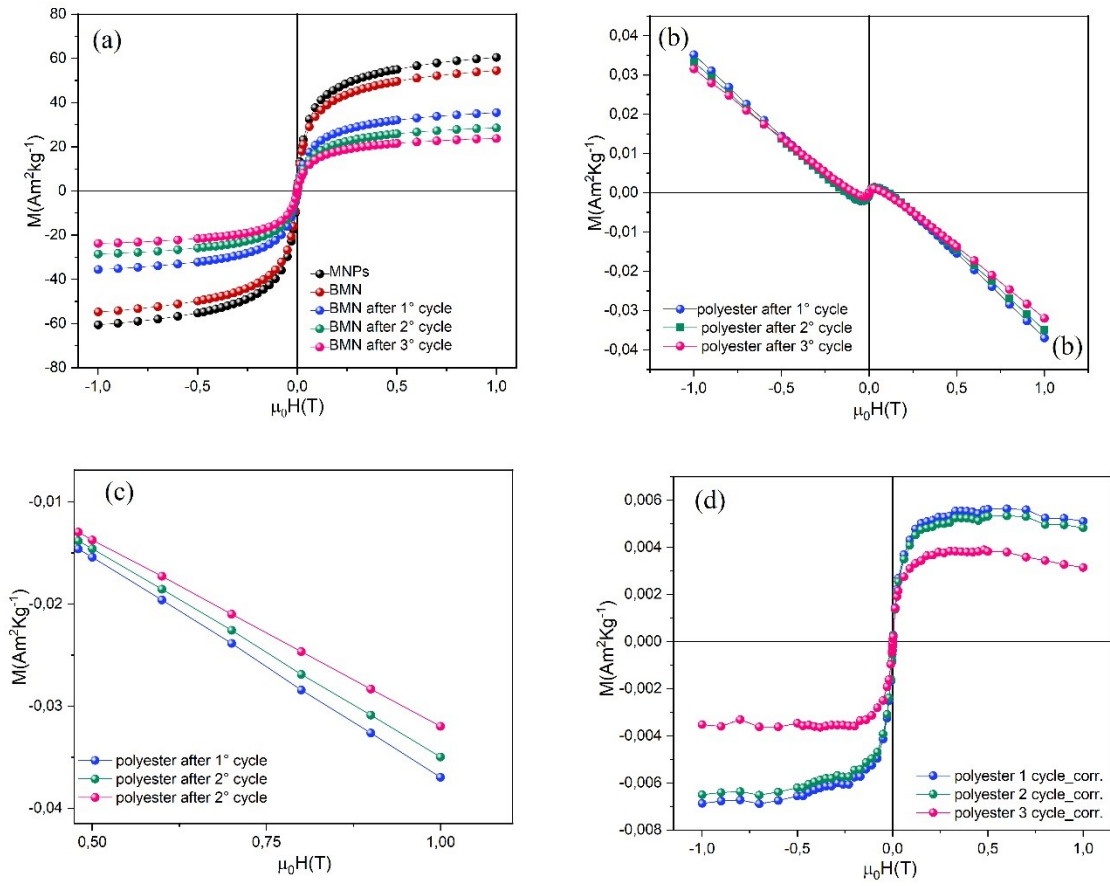


Figure S11: (a) vs M vs H at 300K of MNP, BMN, and MNP_calc after the 1st, 2nd, 3rd reaction cycle, (b) M vs H of the polyester after each cycle at 300K; (c) Diamagnetic phase after each cycle at 300K. (d) M vs H of the polyester after each cycle corrected at 300K

The calculation of the percentage of magnetic nanoparticles (NPs) after each recovery cycle was determined using saturation magnetization data, through the following formula:

$$\%NPs = \frac{Ms_{MNP}}{Ms_{rec}} \times 100 \quad (S1)$$

Ms_{MNP} initial magnetization of bare particles, Ms_{rec} is the saturation magnetization after each recovery cycle.

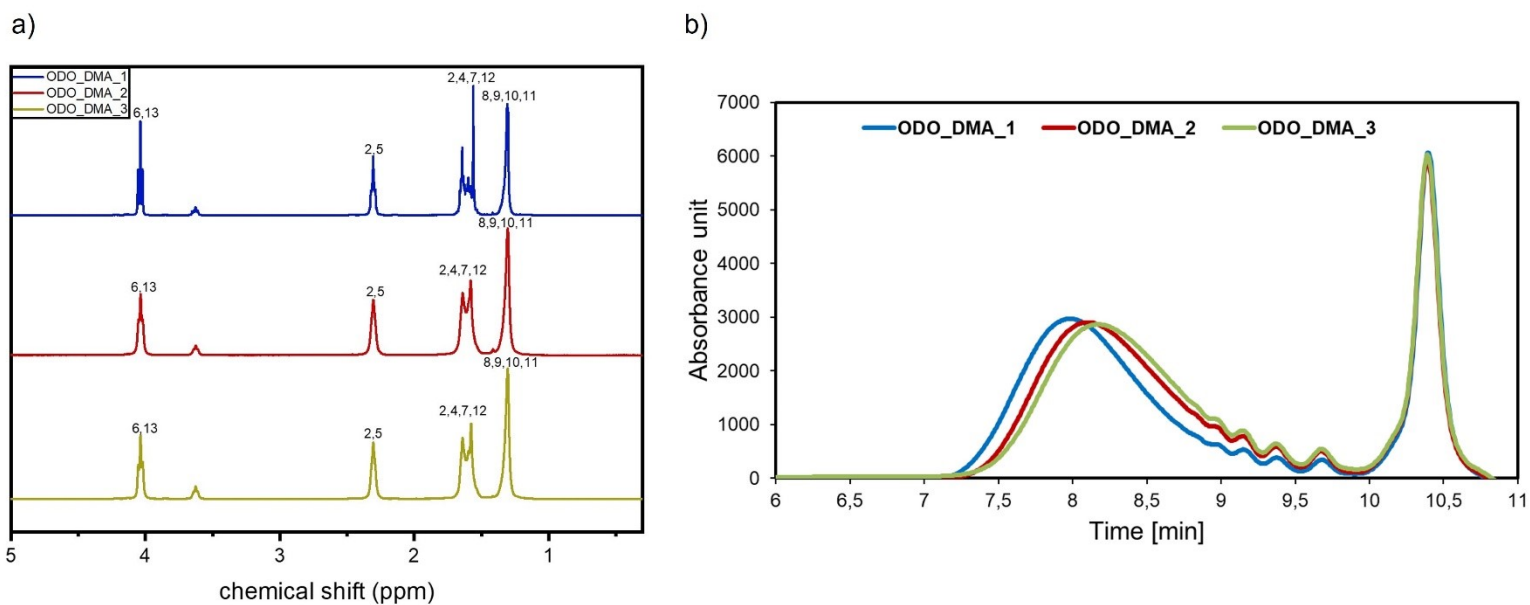


Figure S12: The monitored $^1\text{H-NMR}$ spectra (a) and GPC charts (B) of polycondensation progress over 3 cycles of reaction

Table S1: Comparison between % of monomer conversion and M_n for 3 different cycles of reaction

Reaction cycle	% of monomer conversion	M_n (Da)	M_w (Da)	Dispersity (\bar{M}_w/\bar{M}_n)
DMA_ODO 1 st cycle	92	5600	11000	1.96
DMA_ODO 2 nd cycle	89	4400	7800	1.77
DMA_ODO 3 rd cycle	87	4200	7000	1.66

Bibliography

1. Ficanha AMM, Antunes A, Oro CED, Dallago RM, Mignoni ML. Immobilization of candida antarctica b (calb) in silica aerogel: Morphological characteristics and stability. *Biointerface Res Appl Chem*. 2020;10:6744–56.
2. Jang WY, Sohn JH, Chang JH. Thermally stable and reusable silica and Nano-Fructosome Encapsulated CalB enzyme particles for Rapid Enzymatic Hydrolysis and Acylation. *International Journal of Molecular Sciences*. 2023;24(12):9838.